Theoretical Design of Doubly Bonded Hypervalent Atoms

Hiroaki Kameyama, Yuji Naruse, and Satoshi Inagaki*

Department of Chemistry, Gifu University, 1-1 Yanagido, Gifu 501-1193, Japan

Received January 16, 2007

Molecules that contain a double bond between hypervalent atoms were designed. They included monocyclic five-membered ring molecules $[HCO_2(FPn)_2]^-$ and bicyclic molecules $[HCO_2Pn]_2$ (Pn = Sb, Bi), which contain one and two carboxylato $(HCO_2)^-$ bridges between the doubly bonded pnictogen atoms, respectively. The bicyclic molecules are kinetically and thermodynamically more stable than the monocyclic molecules.

Introduction

The chemistry of hypervalent compounds has attracted the attention of both organic and inorganic chemists over the past half century.[1] Hypervalent molecules are also of broad theoretical and experimental interest because of their unusual geometrical and electronic structures[1,2] and their importance as reactive intermediates in some chemical reactions.[3] Multiple bonds between high-row elements, phosphorus and silicon (see **1** and **2**), were first reported in 1981 by Yoshifuji and co-workers[4a] and by West and co-workers,[4b] respectively. Single bonds between "hypervalent"[5] atoms have been reported for silicon,[6] germanium,[7] and tin[8] (see **3**−**5**). In this paper, we report our theoretical design of stable double bonds between hypervalent atoms.

Results and Discussion

We chose $[SiH_3{=}SiH_3]^{2-}$ and $[PH_2{=}PH_2]^{2-}$ as simple model compounds that contain a double bond between hypervalent atoms. A double bond requires a planar structure. Therefore, we performed calculations for planar $Si_2H_6^{2-}$ and $P_2H_4^{2-}$ at the B3LYP/6-311++G** level.[9] The geometries were optimized for fixed Si−Si−H (or P−P−H) bond angles. The calculations show that $Si_2H_6^{2-}$ has a Si═Si double bond with a Si−Si−H bond angle of around 100°, and there is a bonding π-orbital among the high-lying occupied orbitals and an antibonding π^*-orbital among the low-lying vacant orbitals (Figure 1). The Si−Si bond is dissociated at wider Si−Si−H bond angles. The phosphorus species $P_2H_4^{2-}$ was not shown to have a P═P double bond. The bonding and antibonding π-orbitals are both occupied by electrons with P−P−H bond angles of around 100°, while the P−P bond is dissociated for wider P−P−H bond angles. We performed calculations for $Si_2F_6^{2-}$ and $P_2F_4^{2-}$ to investigate the effects of the electronegativity of the atoms bonded to Si and P. Similar results were obtained for $Si_2F_6^{2-}$. In $P_2F_4^{2-}$, there is a P═P double bond with a P−P−F bond angle of around 100°.

Ar−P=P−Ar

Ar =2,4,6-tri-t-butylphenyl

1

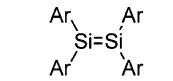

Ar =2,4,6-trimethylphenyl

2

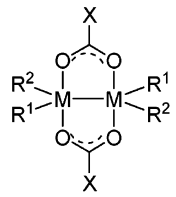

3 M = Si; R^1 = Me, R^2 = $ArCO_2$; X = 2,6-dimethylphenyl
4 M = Ge; R^1 = R^2 = Ph; X = CCl_3
5a M = Sn; R^1 = R^2 = Me; X = CH_2Cl
5b M = Sn; R^1 = R^2 = Me; X = CCl_3
5c M = Sn; R^1 = R^2 = Me; X = CF_3
5d M = Sn; R^1 = R^2 = Ph; X = CH_3

The calculated results suggest some structural features that are important for molecules $X_nM{=}MX_n$ that contain doubly bonded hypervalent atoms. The bond angle M−M−X should be near 100°. We used five-membered ring structures, i.e., the monocyclic (**6**−**13**) and bicyclic (**14**−**21**) molecules. Oxygen atoms were chosen as ring atoms for the electronegative fluorine atoms. A tricoordinate carbon atom (CH) with a vacant p-orbital was chosen as the remaining part of the ring. The vacancy of the p-orbital gives rise to 6π electrons (2π electrons of the double bond and 4π lone pair electrons on the oxygen atoms) in the ring. Fortunately, further stabilization of cyclic molecules or pentagon stability[10] is expected from the cyclic delocalization of the σ-lone pairs on the oxygen atoms through the vicinal

* Corresponding author. E-mail: inagaki@apchem.gifu-u.ac.jp.

(1) (a) Pauling, L. *The Nature of the Chemical Bond*, 3rd ed., Cornell Univ. Press: Ithaca, NY, 1960. (b) Gillespie, R. J. *Molecular Geometry*; Van Nostrand Reinhold: London, 1972. (c) Block, E. *Heteroatom Chemistry*; VCH: New York, 1990. (d) Akiba, K.-y. *Chemistry of Hypervalent Compounds*; Wiley-VCH: New York, 1999.

(2) (a) Kutzelnigg, W. *Angew. Chem., Int. Ed. Engl.* **1984**, *23*, 272. (b) Reed, A. E.; Schleyer, P. V. R. *J. Am. Chem. Soc*. **1990**, *112*, 1434.

(3) Burggraf, L. W.; Davis, L. P. *Chemically Modified Surfaces*; Gordon and Breach Science: New York, 1986; pp 157−187.

(4) (a) Yoshifuji, M.; Shima, I.; Inamoto, N.; Hirotsu, K.; Higuchi, T. *J. Am. Chem. Soc*. **1981**, *103*, 4587. (b) West, R.; Fink, M. J.; Michl, J. *Science* **1981**, *214*, 2140.

(5) The four σ_{MO} bonds are as long as one another.

(6) Recently, Kawashima reported molecules that connect two hypervalent silicon atoms bridged by (thio)carboxylato ligands; see: (a) Kano, N.; Nakagawa, N.; Kawashima, T. *Angew. Chem., Int. Ed.* **2001**, *40*, 3450. (b) Kano, N.; Nakagawa, N.; Shinozaki, Y.; Kawashima, T.; Sato, Y.; Naruse, Y.; Inagaki, S. *Organometallics* **2006**, *24*, 2823. See also ref 17g.

(7) Simon, D.; Häberle, K.; Dräger, M. *J. Organomet. Chem*. **1984**, *267*, 133.

(8) (a) Bangoli, G.; Clemente, D. A. *J. Chem. Soc., Chem. Commun.* **1971**, 311. (b) Faggiani, R.; Johnson, J. P.; Brown, I. D.; Birchall, T. *Acta Crystallogr*. **1978**, *B34*, 3742. (c) Faggiani, R.; Johnson, J. P.; Brown, I. D.; Birchell, T. *Acta Crystallogr*. **1979**, *B35*, 1227. (d) Birchall, T.; Johnson, J. P. *Can. J. Chem*. **1982**, *60*, 934.

(9) *Gaussian 98*, Revision A. 11. 3; Gaussian, Inc.: Pittsburgh, PA, 2002.

10.1021/om0700415 CCC: $37.00 © 2007 American Chemical Society
Publication on Web 10/11/2007

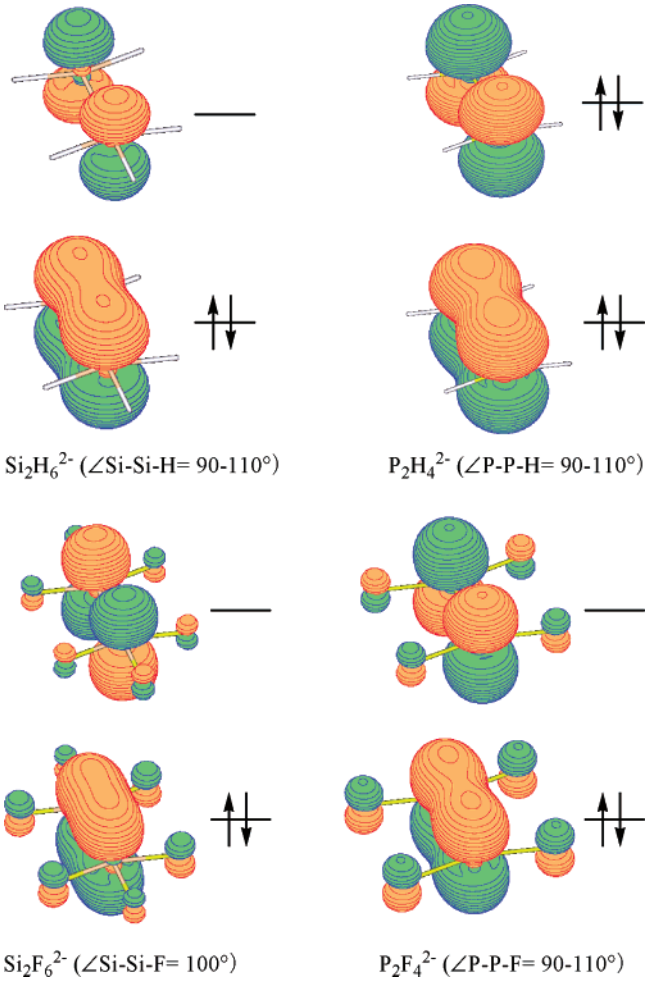

Figure 1. Bonding and antibonding π-orbitals.

σ-bond (Figure 2). The lone pairs are donors. The C−O σ-bond of the carboxylato group and the M−M σ-bond are acceptors. The lone pair orbital (n), the σ^*_{C-O}-orbital, and the σ^*_{M-M}-orbital satisfy the orbital phase continuity conditions:[11,12] the accepting σ^*-orbitals are in-phase and the donating (n) and accepting σ^*-orbitals are in-phase. Thus, the cyclic delocalization of lone pair electrons is enhanced.

Monocyclic Molecules. We optimized the geometries of monocyclic molecules **6**−**9** (M = Si, Ge, Sn, and Pb) and **10**−**13** (Pn = P, As, Sb, and Bi) under the constraint of C_{2v} symmetry at the B3LYP/LANL2DZ level.[9] The C_{2v} geometries are not equilibrium structures for **6**−**9**, as shown by a few imaginary frequencies, but are equilibrium structures for **10**−**13** (Figure 3). There is a double bond between the pnictogen atoms in **10**−**13**. The bonding π-orbital is occupied by electrons, whereas the antibonding π-orbitals are vacant (Figure 4). Calculations for **6**, **7**, **10**, and **11** containing a lighter atom (M = Si, Ge, P, As) at the higher level (B3LYP/6-311++G**) gave similar results, except for a few imaginary frequencies of the C_{2v} geometry of **10**.

We investigated the kinetic and thermodynamic stabilities of **10**−**13**. The calculations suggested that all of the five-membered ring species could isomerize into the three-membered ring species **10a**−**13a** (Figure 5) with low enthalpies of activation:

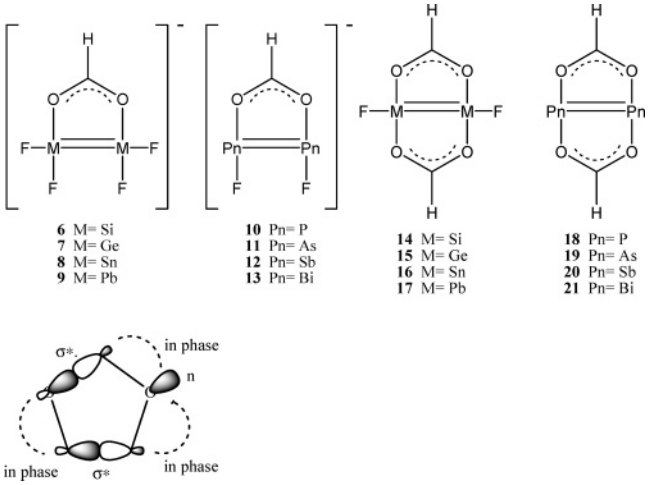

Figure 2. Orbital phase continuity for the pentagon stability.

$\Delta H^{\ddagger}$ = 0.5 kcal/mol for **10**; 3.3 kcal/mol for **11**; 6.3 kcal/mol for **12**; and 6.9 kcal/mol for **13**. Molecules **10**−**13** show slight differences in the thermodynamic stability from the three-membered ring species: ΔH = −2.5 kcal/mol for **10**; 1.5 kcal/mol for **11**; 4.4 kcal/mol for **12**; and 5.8 kcal/mol for **13**. The monocyclic molecules **10**−**13**, which contain a double bond between the pnictogen atoms, are thermodynamically and kinetically unstable and difficult to isolate and characterize.

Bicyclic Molecules. We designed the bicyclic molecules **14**−**21**. Further stabilization is expected from an additional cyclic delocalization of the π- and n-electrons (Figure 2). The geometries of D_{2h} symmetry were optimized at the B3LYP/LANL2DZ level (Figure 6).

The D_{2h} geometries of **14**−**17**, which contain double bonds between the atoms in group 14, have a few imaginary frequencies like the monocyclic geometries **6**−**9**. Thus, they are not equilibrium geometries. On the other hand, molecules **19**−**21** (Pn = As, Sb, Bi) are at local minima, whereas **18** (Pn = P) is the transition state of the rapid degenerate rearrangement with an enthalpy of activation $\Delta H^{\ddagger}$ = 0.88 kcal/mol for diphosphirene **18a** with normal valency where the formyl groups are on the sides syn to the P═P bond. Molecules **19**−**21** have a double bond between heavy atoms. The HOMO is the bonding π-orbital and the LUMO is the antibonding π-orbital (Figure 7).

The bicyclic molecules **19**−**21** isomerize to dipnictogenenes **19a**−**21a** (Figure 8), respectively, as was suggested by the earlier result that the C_{2v} geometry of **18** is the transition state of the diphosphirene **18a**. Surprisingly, the products are syn,anti-conformers. One formyl group is on the syn side of the Pn═Pn bond, whereas the other is on the anti side. The syn,syn-conformers were not located at local energy minima. These results suggest that **19**−**21** are kinetically stable. The enthalpies of activation of isomerization and the energy differences between **19**−**21** and the products were calculated at the B3LYP/LANL2DZ (B3LYP/6-311++G**) levels. The enthalpies of activation are appreciable (12.7 (10.9) kcal/mol for **19**) and outstanding (18.3 kcal/mol for **20**; 21.9 kcal/mol for **21**). Molecules **19**−**21** are thermodynamically more stable than the products, as shown by their energy differences (ΔH = 10.6 (8.9) kcal/mol for **19**; 16.3 kcal/mol for **20**; 19.4 kcal/mol for **21**).

(10) (a) Ma, J.; Hozaki, A.; Inagaki, S. *Inorg. Chem.* **2002**, *41*, 1876. (b) Ma, J.; Hozaki, A.; Inagaki, S. *Phosphorus, Sulfur Silicon* **2002**, *177*, 1705.

(11) Fukui, K.; Inagaki, S. *J. Am. Chem. Soc.* **1975**, *97*, 4445.

(12) Inagaki, S.; Kawata, H.; Hirabayashi, Y. *Bull. Chem. Soc. Jpn.* **1982**, *55*, 3724.

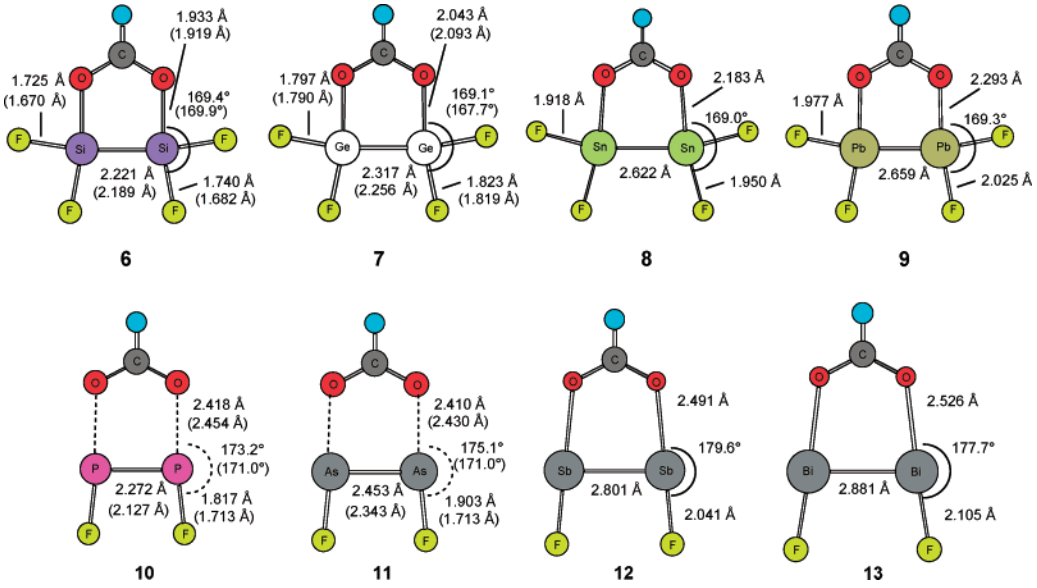

Figure 3. C_{2v} geometries optimized at the B3LYP/LANL2DZ (B3LYP/6-311++G**) level.

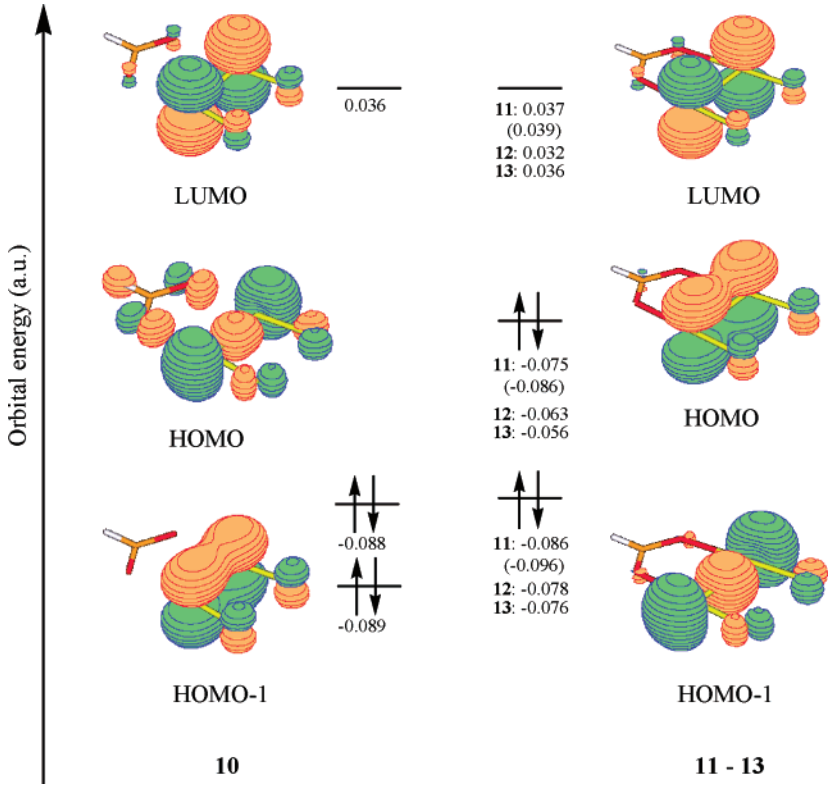

Figure 4. High-lying molecular orbitals and the LUMO of **10**−**13** calculated at the B3LYP/LANL2DZ (B3LYP/6-311++G**) level.

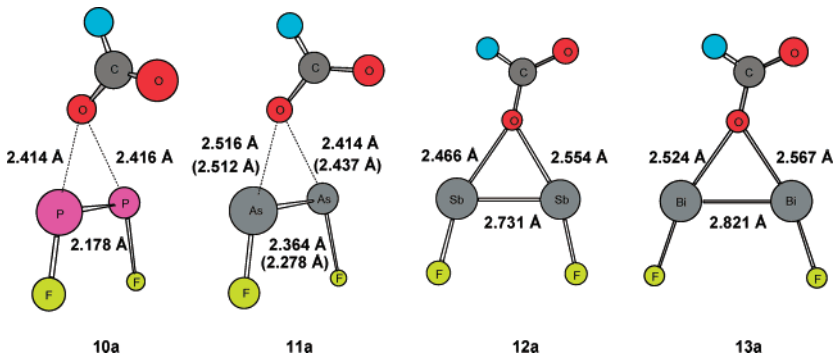

Figure 5. Geometries of the products of the rearrangement of **10**−**13** optimized at the B3LYP/LANL2DZ (B3LYP/6-311++G**) level.

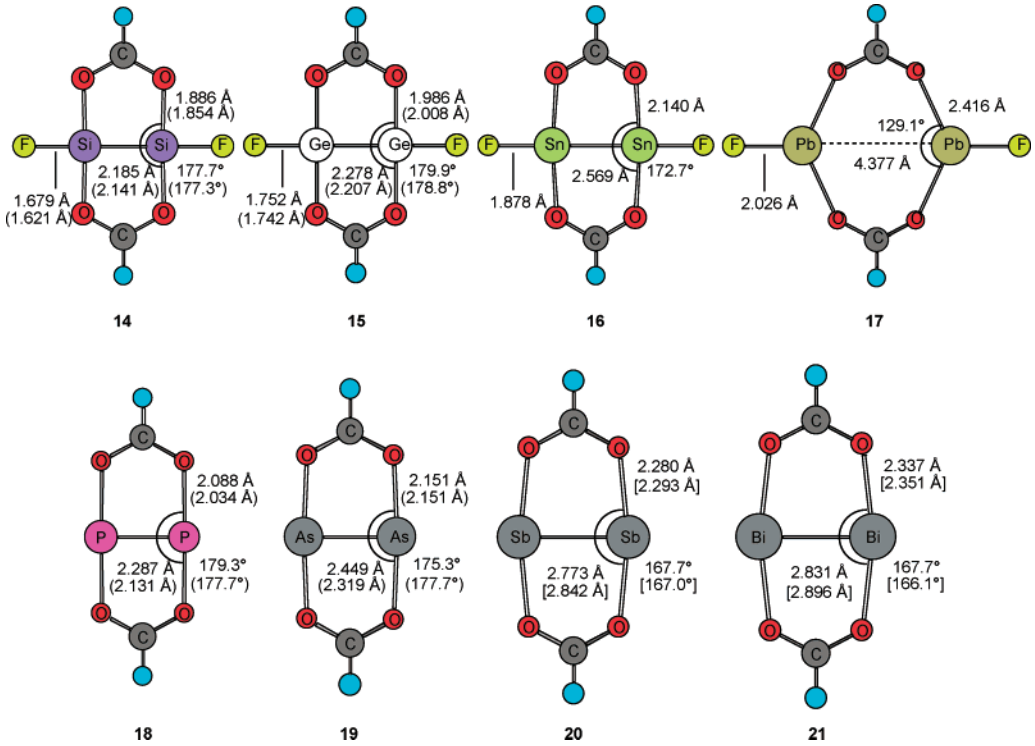

Figure 6. Geometries of **14**−**21** optimized under the constraint of the D_{2h} symmetry at the B3LYP/LANL2DZ (B3LYP/6-311++G**) [MP2/LANL2DZ] level.

Table 1. Interbond Energies (IBE)[17] between the Geminal Bonds and Hybrid Orbitals (HO) of 8 and 12 Calculated at the RHF/LANL2DZ Level Using the B3LYP/LANL2DZ-Optimized Geometries.

	IBE (au)		HO[a]	
	$\sigma_{M(Pn)M(Pn)}-\sigma^*_{M(Pn)O}$	$\sigma_{M(Pn)O}-\sigma^*_{M(Pn)M(Pn)}$	$\sigma_{M(Pn)M(Pn)}$	$\sigma_{M(Pn)O}$
8 (M = Sn)	0.310	−0.190	$sp^{0.59}$	$sp^{97.9}$
12 (Pn = Sb)	0.000	0.000	$sp^{5.11}$	$sp^{21.8}$

[a] Hybrid orbitals on M(Pn).

We performed further calculations for **19** at the MP2/6-311++G** and MP2/LANL2DZ levels and for **20** and **21** at the MP2/LANL2DZ level. The MP2 calculations supported the results of the DFT calculations, which showed that **20** and **21** are kinetically and thermodynamically stable molecules (Figure 9).[13] However, a local energy minimum was not found for **19** at the MP2 level.

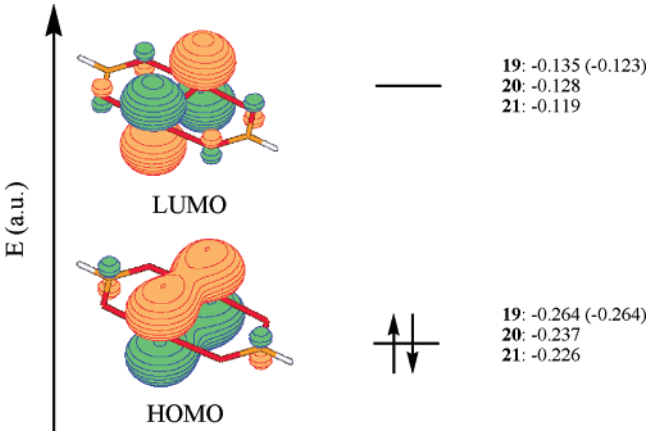

Figure 7. HOMO (bonding π-orbital) and LUMO (antibonding π^*-orbital) of **19**−**21** calculated at the B3LYP/LANL2DZ (B3LYP/6-311++G**) level.

There were clear differences between the elements in groups 14 and 15. Neither monocyclic nor bicyclic molecules containing a double bond between the hypervalent atoms were located as energy minima for group 14 elements. The bonding−antibonding property of the $\sigma-\sigma^*$ interaction between the geminal ring bonds was previously proposed to indicate ring strain.[14] We subjected **8** (M = Sn) and **12** (Pn = Sb) to the bond model analysis.[15] According to the calculated interbond energy (IBE)[16,17] (Table 1), the geminal $\sigma_{PnPn}-\sigma^*_{PnO}$ and $\sigma_{PnO}-\sigma^*_{PnPn}$ interactions in **12** (Pn = Sb) are nonbonding (Figure 10), whereas the antibonding property (0.310 au) of $\sigma_{MM}-\sigma^*_{MO}$ interaction is greater than the bonding property (−0.190 au) of the $\sigma_{MO}-\sigma^*_{MM}$ interaction in **8** (M = Sn). The predominance of the antibonding property strains the ring. The hybrid orbitals for σ_{MM} of **8** (M = Sn) have higher s-character than those for σ_{PnPn} of **12** (Table 1) due to the low s-character of the hybrid orbital on M for the M−O bond (M = Sn) and the high s-character of the lone pair on Pn(=Sb). The high s-character of σ_{MM} (M =

(13) We also calculated the ΔG and $\Delta G^{\ddagger}$ values for the reactions of **20** and **21** (Figure 9) at 298.15 K, 1 atm, at the B3LYP/LANL2DZ (B3LYP/6-311++G**) [MP2/LANL2DZ] level. The $\Delta G^{\ddagger}$ values (17.3 kcal/mol [17.9 kcal/mol] for **20** and 21.7 kcal/mol [21.3 kcal/mol] for **21**) and the ΔG values (14.1 kcal/mol [14.2 kcal/mol] for **20** and 17.7 kcal/mol [17.3 kcal/mol] for **21**) do not significantly differ from the $\Delta H^{\ddagger}$ and ΔH values (see the Supporting Information).

(14) (a) Inagaki, S.; Goto, N. *J. Am. Chem. Soc.* **1987**, *109*, 3234. (b) Inagaki, S.; Goto, N.; Yoshikawa, K. *J. Am. Chem. Soc.* **1991**, *113*, 7144. (c) Inagaki, S.; Yoshikawa, K.; Hayano, Y. *J. Am. Chem. Soc.* **1993**, *115*, 3706. (d) Inagaki, S.; Ishitani, Y.; Kakefu, T. *J. Am. Chem. Soc.* **1994**, *116*, 5954.

(15) For the bond model analysis, see (a) Inagaki, S.; Ikeda, H. *J. Org. Chem.* **1998**, *63*, 7820. (b) Iwase, K.; Inagaki, S. *Bull. Chem. Soc. Jpn.* **1996**, *69*, 2781. For another method of the bond model analysis, see: (c) Ikeda, H.; Inagaki, S. *J. Phys. Chem. A* **2001**, *47*, 10711.

(16) Inagaki, S.; Yamamoto, T.; Ohashi, S. *Chem. Lett.* **1997**, 977.

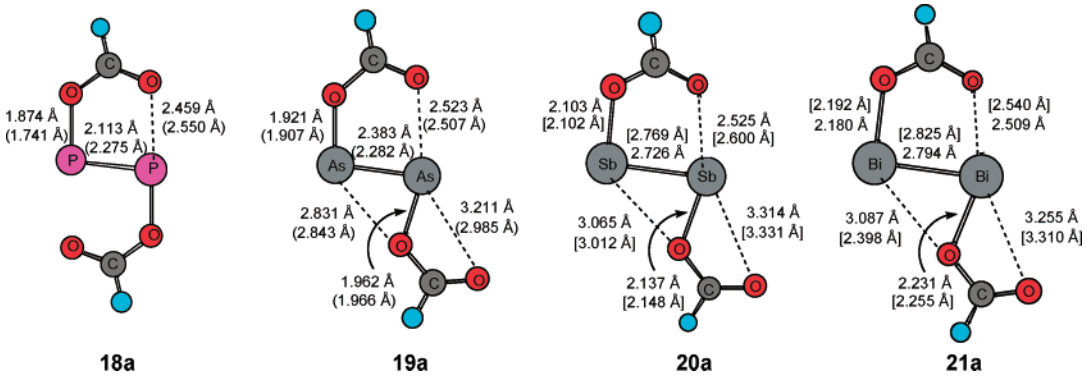

Figure 8. Geometries of **18a**−**21a** optimized at the B3LYP/LANL2DZ (B3LYP/6-311++G**) [MP2/LANL2DZ] level.

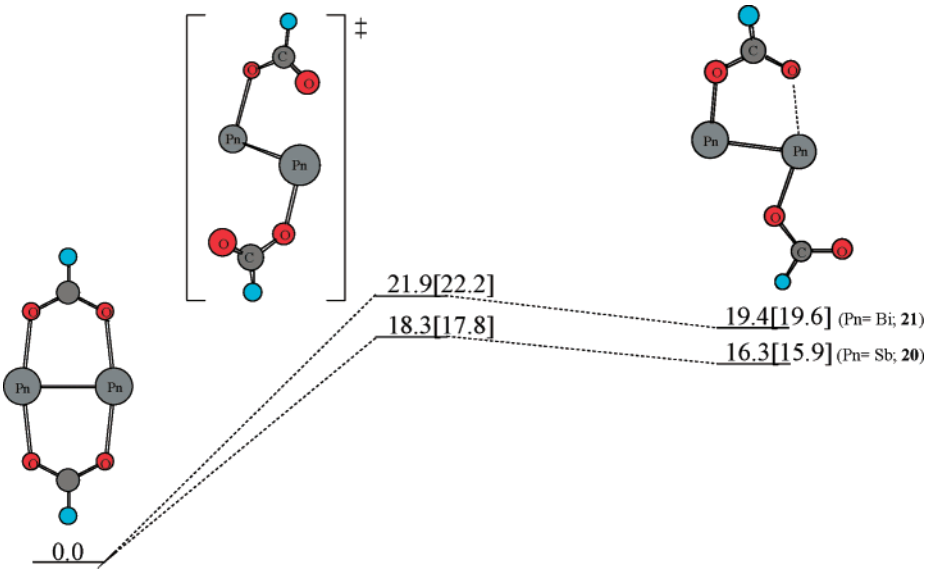

Figure 9. Enthalpies of activation (kcal/mol) of the isomerization and thermodynamic stabilities of **20** and **21** at the B3LYP/LANL2DZ [MP2/LANL2DZ] level.

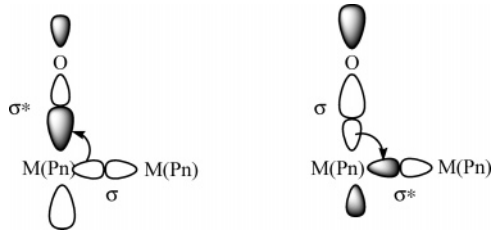

Figure 10. Geminal bond orbital interactions.

Sn) is a factor for the antibonding property of the geminal delocalization[14] and strains the ring of **8**.

Conclusion

We designed some molecules with a double bond between hypervalent atoms. Monocyclic five-membered ring molecules containing hypervalent Sb and Bi atoms (**12**, **13**) with a carboxylato $(HCO_2)^-$ bridge between them are kinetically and thermodynamically unstable because of the low barrier for isomerization and the small energy difference from the products. Bicyclic molecules **20** and **21**, containing the hypervalent Sb and Bi atoms with two carboxylato bridges, are kinetically and thermodynamically stable. The barriers for the isomerization are reasonable, and the energies are significantly lower than those of the products. The corresponding monocyclic and bicyclic molecules containing atoms of the group 14 elements were not located at the local energy minima. Finally, the bicyclic molecules **20** and **21**, which contain a double bond between the hypervalent Sb or Bi atoms, are recommended for synthesis as a first target. Important factors in stabilizing the double bond between the hypervalent atoms for group 15 elements are effective cyclic delocalizations of π and lone pair electrons and low ring strain.

Acknowledgment. We gratefully acknowledge the financial support from Gifu University.

Supporting Information Available: Calculated structures with the energies. This material is available free of charge via the Internet at http://pubs.acs.org.

OM0700415

(17) IBE is derived as follows: $IBE_{ij} = P_{ij}(H_{ij} + F_{ij})$, where P_{ij}, H_{ij}, and F_{ij} are the elements of the density, Fock, and core Hamiltonian matrices of the bond orbitals, respectively. For its application, see: (a) Inagaki, S.; Ohashi, S.; Kawashima, T. *Org. Lett.* **1999**, *1*, 1145. (b) Inagaki, S.; Ikeda, H.; Kawashima, T. *Tetrahedron Lett.* **1999**, *40*, 8893. (c) Ikeda, H.; Naruse, Y.; Inagaki, S. *Chem. Lett.* **1999**, 363. (d) Naruse, Y.; Hayashi, A.; Sou, S.; Ikeda, H.; Inagaki, S. *Bull. Chem. Soc. Jpn.* **2001**, *74*, 245. (e) Ikeda, H.; Ushioda, N.; Inagaki, S. *Chem. Lett.* **2001**, 166. (f) Ikeda, H.; Kato, T.; Inagaki, S. *Chem. Lett.* **2001**, 270. (g) Naruse, Y.; Inagaki, S.; Kano, N.; Nakagawa, N.; Kawashima, T. *Tetrahedron Lett.* **2002**, *43*, 5759. (h) Naruse, Y.; Sugiura, M.; Inagaki, S. *Phosphorus, Sulfur, Silicon* **2003**, *178*, 2447. (i) Otani, Y.; Nagae, O.; Naruse, Y.; Inagaki, S.; Ohno, M.; Yamaguvchi, K.; Yamamoto, G.; Uchiyama, M.; Ohwada, T. *J. Am. Chem. Soc.* **2003**, *125*, 15191. (j) Naruse, Y.; Hayashi, Y.; Inagaki, S. *Tetrahedron Lett.* **2003**, *44*, 8509. (k) Yasui, M.; Naruse, Y.; Inagaki, S. *J. Org. Chem.* **2004**, *69*, 7246. (l) Naruse, Y.; Suzuki, T.; Inagaki, S. *Tetrahedron Lett.* **2005**, *46*, 6937. (m) Naruse, Y.; Ma, J.; Takeuchi, K.; Nohara, T.; Inagaki, S. *Tetrahedron* **2006**, *62*, 4491. (n) Naruse, Y.; Fukasawa, S.; Ota, S.; Deki, A.; Inagaki, S. *Tetrahedron Lett.* **2007**, *48*, 817.